This article was downloaded by:
On: *26 January 2011*
Access details: *Access Details: Free Access*
Publisher *Taylor & Francis*
Informa Ltd Registered in England and Wales Registered Number: 1072954 Registered office: Mortimer House, 37-41 Mortimer Street, London W1T 3JH, UK

Liquid Crystals
Publication details, including instructions for authors and subscription information:
http://www.informaworld.com/smpp/title~content=t713926090

Optical probing of thin liquid crystal layers using the prism-coupling technique

C. R. Lavers[a]
[a] Optoelectronics Research Centre, University of Southampton, Southampton, England

To cite this Article Lavers, C. R.(1992) 'Optical probing of thin liquid crystal layers using the prism-coupling technique', Liquid Crystals, 11: 6, 819 — 832
To link to this Article: DOI: 10.1080/02678299208030687
URL: http://dx.doi.org/10.1080/02678299208030687

PLEASE SCROLL DOWN FOR ARTICLE

Full terms and conditions of use: http://www.informaworld.com/terms-and-conditions-of-access.pdf

This article may be used for research, teaching and private study purposes. Any substantial or systematic reproduction, re-distribution, re-selling, loan or sub-licensing, systematic supply or distribution in any form to anyone is expressly forbidden.

The publisher does not give any warranty express or implied or make any representation that the contents will be complete or accurate or up to date. The accuracy of any instructions, formulae and drug doses should be independently verified with primary sources. The publisher shall not be liable for any loss, actions, claims, proceedings, demand or costs or damages whatsoever or howsoever caused arising directly or indirectly in connection with or arising out of the use of this material.

LIQUID CRYSTALS, 1992, VOL. 11, No. 6, 819–832

Optical probing of thin liquid crystal layers using the prism-coupling technique

by C. R. LAVERS
Optoelectronics Research Centre,
University of Southampton, Southampton SO9 5NH, England

(*Received 12 June 1991; accepted 17 November 1991*)

Prism-coupling work in polymer aligned liquid crystal layers is presented with special emphasis being placed on the ferroelectric chiral smectic C phase, of interest to electro-optic device fabrication. Experimental results as a function of temperature, wavelength and DC applied voltage are presented, together with a study of sp mixing which may have potential device applications as well as being an elegant technique with which to establish the optical dielectric tensor configuration in thin, aligned liquid crystal layers.

Downloaded At: 12:36 26 January 2011

1. Introduction

Prism-coupling as a means of probing thin layers to obtain information on the optical dielectric tensor parameters has been known for a long time. The Otto [1] and Kraetschmann–Raether configurations [2] have been well-documented as reliable methods for coupling light into thin layers. If the metal layer in the Kraetschmann geometry is replaced by indium tin oxide (ITO) dielectric coated layers than leaky Fabry–Perot optical guided modes may be propagated in a symmetric system composed of a prism/ITO/aligning layer/liquid crystal/aligning layer/ITO/prism multi-layered structure. Optical guided modes obtained as a function of the angle of incidence may be compared to theory generated from a formalism of Fresnel's equations and the distribution of the electric field profiles for each guided mode acts as a refractive index probe across the system. From such a system it is possible to accurately map important structural parameters, such as the layering structure and DC applied field layer distortion, necessary for future ferroelectric liquid crystal device design.

2. Outline of the technique

To analyse the optical dielectric parameters of a multi-layered structure it is necessary to measure the reflection properties of the system. The prism-coupling technique is used here where optical guided modes are propagated in thin liquid crystal layers [3–7]. Guided modes may only be excited when the momenta of the impinging radiation and the particular guided mode are matched. These sharp dips in the reflectivity spectra are sensitive to the optical properties of the layer in question. Coupling is achieved by means of a high refractive index pyramid where the wavevector along the interface is given by

$$k_z = nk \sin \theta,$$

where k_z is the component of the momentum along the interface in the plane of propagation, n is the refractive index of the glass pyramid, $k = 2\pi/\lambda = \omega/c$ where k is the

0267–8292/92 $3·00 © 1992 Taylor & Francis Ltd.

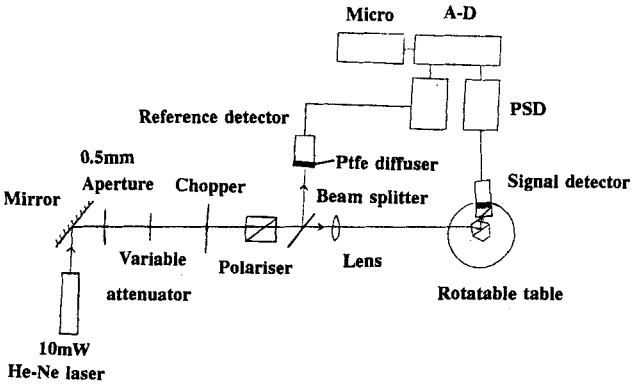

Figure 1. Experimental system.

momentum of the incident photon in free space and is also written in terms of the angular frequency and velocity of light in vacuum, λ is the wavelength of the incident radiation and θ is the angle of incidence, that is the angle between the incident beam and the normal to the interface. Clearly by altering θ it is possible to couple light into different optical guided modes of the system. For an accurate optical determination of the material parameters the experiment is simplified if only two orthogonal polarizations of incident radiation, transverse magnetic (TM or p-polarized) and transverse electric (TE or s-polarized) are used. Monochromatic light is provided by a helium–neon (He–Ne) laser at 632·8 nm; the experimental arrangement is shown in figure 1.

2.1. *Cell fabrication*

Fabrication of aligned thin film cells is the most crucial stage in the experiment. In our geometry conventional glass plates are replaced by high refractive index pyramids, this allows us to probe the optical dielectric tensor configuration in two orthogonal orientations with two incident polarizations (see figure 2). Several important processes are involved with the fabrication.

(i) Cleaning is achieved by refluxing the pyramids in 1,1,1-trichloroethane for 1 hour and then refluxing them in isopropyl alcohol for another hour.
(ii) Indium tin oxide is sputtered onto the base of the pyramids in a Nordiko sputterer to produce a uniform isotropic layer.
(iii) Nolimid 32, a polymer alignment layer, is spun on to the substrates at 3000 rpm for 60 s and soft baked at 80°C for 10 min. The pyramids are then rubbed using a buffing wheel of nylon cloth unidirectionally and hard baked at 200°C for 1 hour.

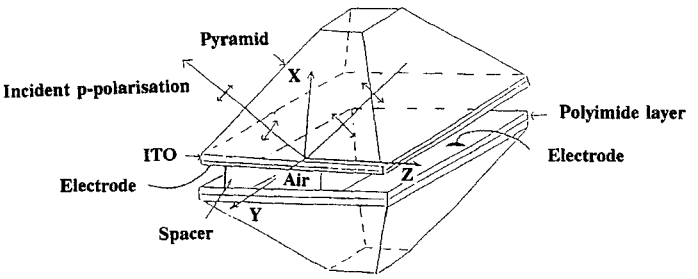

Figure 2. The assembled cell.

Downloaded At: 12:36 26 January 2011

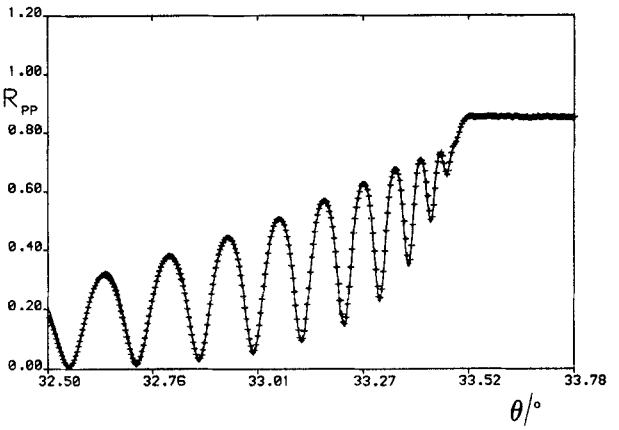

Figure 3. Experimental reflectivity data (+) compared with theory (——) for a pyramid/indium tin oxide/polymer /air/polymer/indium tin oxide/pyramid configuration for TM-polarization at 550 nm.

At each subsequent stage of material deposition reflectivity spectra are taken and by comparison of data with theoretically generated curves the optical parameters are obtained. An experimental reflectivity curve compared with theory is shown for a pyramid/indium tin oxide/polymer/air/polymer/indium tin oxide/pyramid configuration in figure 3.

Downloaded At: 12:36 26 January 2011

2.2. *Liquid crystal cell assembly*

Clear mylar is used to space the pyramids apart and the cell is constructed in a clean room with laminar flow as the trapping of dust particles between the cell surfaces has several serious problems associated with it. For example, poor alignment which inhibits the formation of large ferroelectric domains, severe wedging of the cell which disrupts the optical guided mode structure and electrical breakdown across the dust particle which significantly reduces the lifetime of the cell. The sample surfaces are exposed in the clean room for as little time as possible in an effort to minimize contamination. The two prism faces are then brought into contact; the assembled cell is shown in figure 2. It is possible to place the double prism system in a gimballed arrangement and for it to be rotated about the vertical axis as shown. Measurements are taken in two orthogonal orientations. If the plane of incident polarization lies in the xz plane with the major optic axis (extraordinary axis) of the liquid crystal parallel with the z axis we call this the horizontal orientation. If, however, the sample is rotated about the vertical axis by 90° so that the major optic axis is now along the y axis and hence perpendicular to the incident plane of polarized light then this is the vertical orientation. The assembled cell is enclosed in a temperature controlled oven and is heated until it is above the isotropic phase transition for the liquid crystal under study and then filled by capillary action.

3. Modelling method

The modelling method used calculates theoretical reflectivities as a function of angle of incidence for a multi-layered biaxial media. The multi-layered system is considered as a series of uniform biaxial slabs of dielectric material, where each layer thickness is much less than the wavelength of the incident light. The liquid crystal layer is modelled as 91 layers of equal thickness, this allows a reasonably good approximation to a continuum model of the liquid crystal director configuration. A scattering

matrix formalism is used to overcome instabilities in the more conventional transfer matrix method developed by Berreman and Scheffer [8] and Azzam and Bashara [9]. Both methods take account of the reflection and transmission coefficients at each interface between successive media and use Fresnel's equations. Occasionally the transfer matrix method is unstable above a critical angle due to rapidly decaying and growing evanescent fields. The scattering matrix method, firstly developed by Ko and Sambles [10], couples the incoming fields at any given interface to the outgoing fields by a matrix which is implicitly stable for all incident angles.

4. Simple temperature dependent results without an applied electric field

The first ferroelectric material to be investigated thoroughly using this technique was the BDH (now Merck, Poole) mixture MIX 783. In the isotropic phase only one angle scanned reflectivity plot is necessary to allow a unique determination of the refractive index and cell thickness.

Nematic phase

In a cell thin enough to suppress the bulk chirality reflectivity data was taken for incident TE polarized radiation at 101°C with the cell in the horizontal orientation. Optical guided modes were then observed to propagate in the liquid crystal layer (see figure 4). A simple uniaxial model of the optical dielectric tensor was used to fit the data with the optic axis in the plane of incidence throughout the cell.

Smectic A phase

In the smectic A phase there is no significant change of the structural form of the optical guided modes. Again the simple uniaxial model of the optical dielectric tensor was sufficient to fit the data with the additional imposition of S_A layering.

Chiral smectic C phase

On entering the S_C^* phase there was no apparent structural change in either the TE or TM modes of the system, however monitoring TE light output for TM light incident or TM light output for TE light incident, sharp peaks in the reflectivity spectra were

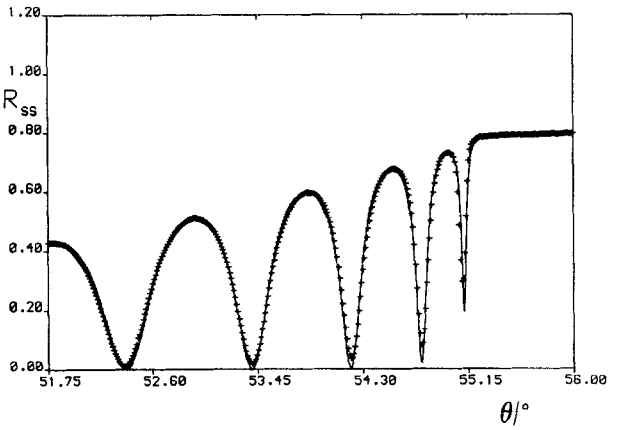

Figure 4. Experimental reflectivity data (+) compared with theory (——) for a cell of MIX 783 in the nematic phase at 101°C with incident TE-polarization and the optic axis in the plane of incidence.

Downloaded At: 12:36 26 January 2011

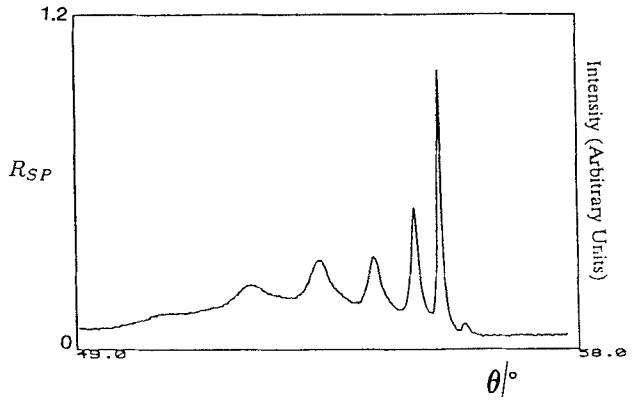

Figure 5. Experimental reflectivity data (——) taken from a 3·5 μm MIX 783 cell just into the S_C^* phase at 59°C, with the optic axis in the plane of incidence.

observed. A typical sp-mixed or Rsp reflectivity scan as a function of angle of incidence is shown for data just below the S_A to S_C^* transition in figure 5. These sp-mixed modes are caused by tilting of the optic axis out of the incident light plane. Off diagonal elements are then non-zero and cause coupling between pure polarization fields and consequently modes are excited of a mixed polarization, TEM mixed modes. The reflectivity data is significantly more complicated as a result of this and we no longer have two orthogonal sets of optical modes of the system. The ferroelectric liquid crystal layer converts s to p polarized light or visa versa with a typical conversion factor at room temperature of about 4 per cent.

4.1. *Optical verification of the chevron model*

Many theoretical models were tried in an attempt to reconcile the temperature dependent data with theory. The best comparison or fit was achieved using a uniformly twisted uniaxial slab model, optically equivalent to the chevron model detected using X-ray scattering by Clark and Rieker [11]. In the chevron model [12] the director axis stays flat in the plane of the surface across the cell. Optically this is equivalent to a uniform slab of dielectric with the major optic axis twisted from the z axis by a constant in-plane tilt angle χ_0 in the yz plane. The smectic layers form from the two surfaces symmetrically as shown in figure 6. The chevron model has a uniform value of in-plane tilt χ_0 and a uniform value of out-of-plane tilt, τ_0. Out-of-plane tilt is simply tilt of the optic axis in the xz plane away from the z axis. Modelling the ferroelectric liquid crystal layer in this way gave reasonable fits to the data. A typical fit is shown for TE modes in figure 7; the data was taken in the vertical orientation at room temperature. Room temperature data is clearly of much interest because most experimental optoelectronics devices will operate in this temperature regime.

4.2. *Boundary layers*

Unfortunately sp-mixing is predicted incorrectly. The intensities and shapes of the predicted sp-mixing modes are wrong. An introduction of a 0·2 μm boundary region at both interfaces with a symmetric in-plane tilt profile (optic axis tilted away from the z axis in the yz plane) gave a close fit to the data as shown in figure 8. However, the second theoretical sp-mode of the system which is more sensitive to the surface region than the

Downloaded At: 12:36 26 January 2011

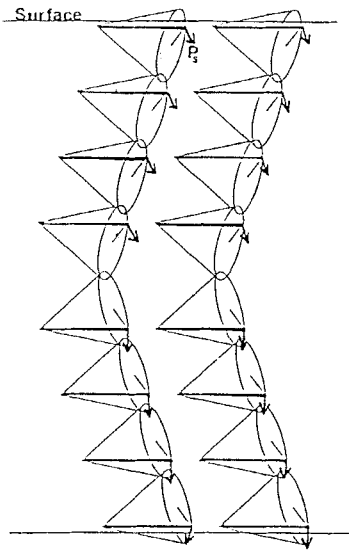

Figure 6. The chevron layer structure.

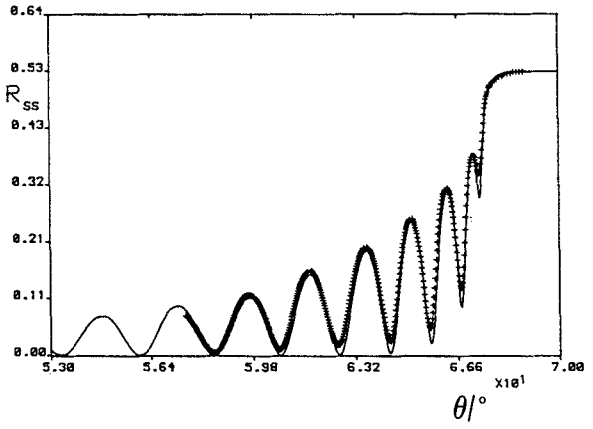

Figure 7. Experimental reflectivity data (+) compared with theory (——) for the ferroelectric liquid crystal MIX 783 at room temperature for TE-polarization with the optic axis perpendicular to the plane of incidence fitted with the chevron layer model.

first order mode is wrong. Secondly the first sp-mode below the critical angle cut-off has split in the theoretically generated curve, this is not observed experimentally. Modelling suggested that the out-of-plane tilt profile at the boundary surfaces might be non-planar [4], this was entirely consistent with the non-uniform surface in-plane tilt profile required to give good agreement between theory and data. This so called boundary layer profile has been verified by conventional optical polarized microscopy for the material SCE 3 independently by Anderson *et al.* [13] and Elston [14]. Although conventional optical polarized microscopy is able to give some information on the optical dielectric tensor profile, the prism-coupling technique is able to probe specific spatial distributions of index across the cell [5] and in the case of cells formed with orthogonal alignment surfaces it was possible to establish the surprising planarity of the director field [15]. A modelling method combining a changing in-plane tilt with

Downloaded At: 12:36 26 January 2011

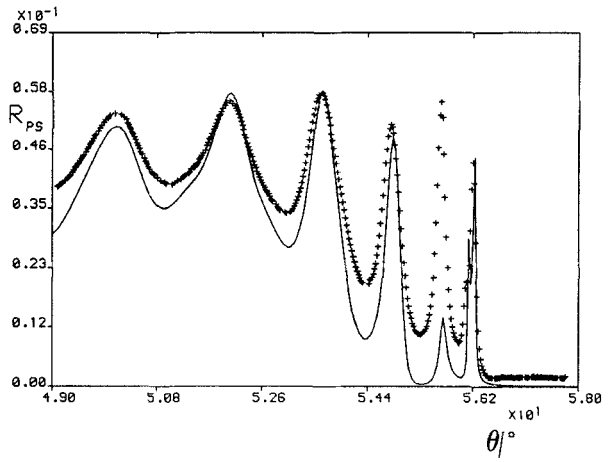

Figure 8. Sp-mixed experimental reflectivity data (+) compared with theory (——) at room temperature in the S_C^* phase with a theoretical model incorporating only symmetric in-plane tilt.

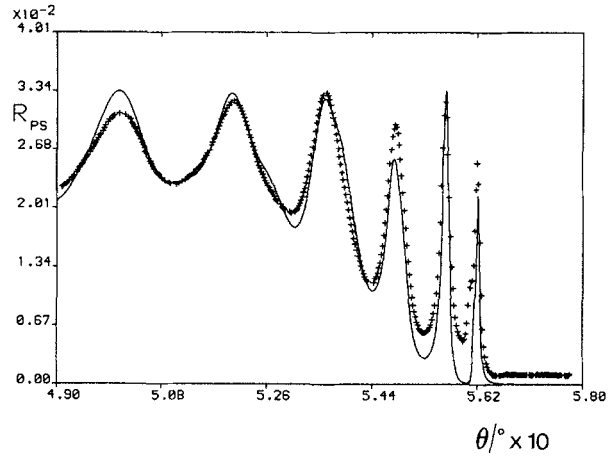

Figure 9. Sp-mixing experimental reflectivity data (+) compared with theory (——) at room temperature in the S_C^* phase with a theoretical model incorporating out-of-plane tilt as well as in-plane tilt.

rotations about the smectic cone for out-of-plane tilt at the surfaces (pretilt) gave the best model of all shown in figure 9. The full in-plane tilt/out-of-plane tilt profile is shown in figure 10.

4.3. *Comments on optical biaxiality and temperature dependent in-plane tilt values*

Significant biaxiality ($\varepsilon_2 - \varepsilon_3 \geqslant 0{\cdot}004$) causes theoretical sp-mode splitting which is never observed experimentally. So a uniaxial chevron model with thin boundary layers gives good comparisons between the data at all temperatures in the S_C^* range, consistent with a small out-of-plane pretilt occurring at the two aligning interfaces. From comparisons between theory and data in-plane tilt values as a function of temperature may also be obtained. The tilt angle may be fitted to a simple Landau expansion given by

$$\chi_0 = \alpha(T_C - T)^\beta$$

Downloaded At: 12:36 26 January 2011

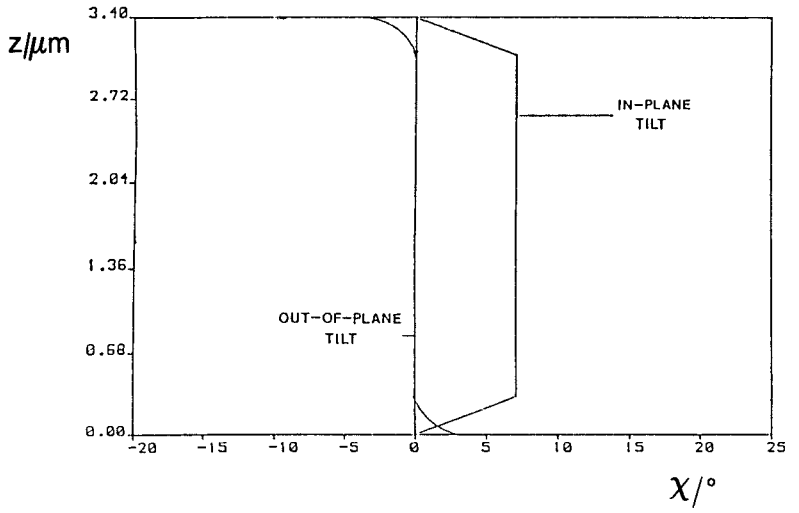

Figure 10. In-plane/out-of-plane tilt profiles.

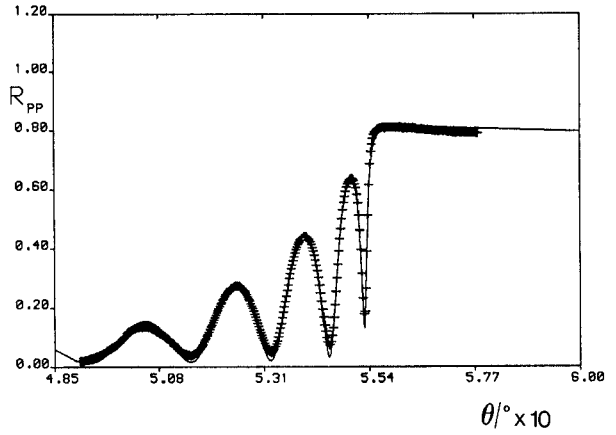

Figure 11. Room temperature SCE 8 experimental reflectivity data (+) compared with theory (——) fitted with the chevron model with the optic axis in the plane of incidence.

where $\alpha = 1{\cdot}47°$, $\beta = 0{\cdot}46 \pm 0{\cdot}01$, T_C is the Curie temperature and T is the temperature of the system [5]. This optical probing technique has also been used for several different liquid crystal materials such as SCE8 and again good agreement between theory and data may be obtained at room temperature (see figure 11).

5. Wavelength characterization

Optical dielectric constants over the visible region of the spectrum were obtained using excitation of leaky Fabry–Perot optical guided modes as described previously. Varying λ allows the k vector to be changed and hence the angles necessary to satisfy the momentum matching conditions. The experimental arrangement is shown in figure 12, a monochromator is provided to scan through the incident wavelength, and photomultiplier tubes are used to detect both signal and reference beams.

Downloaded At: 12:36 26 January 2011

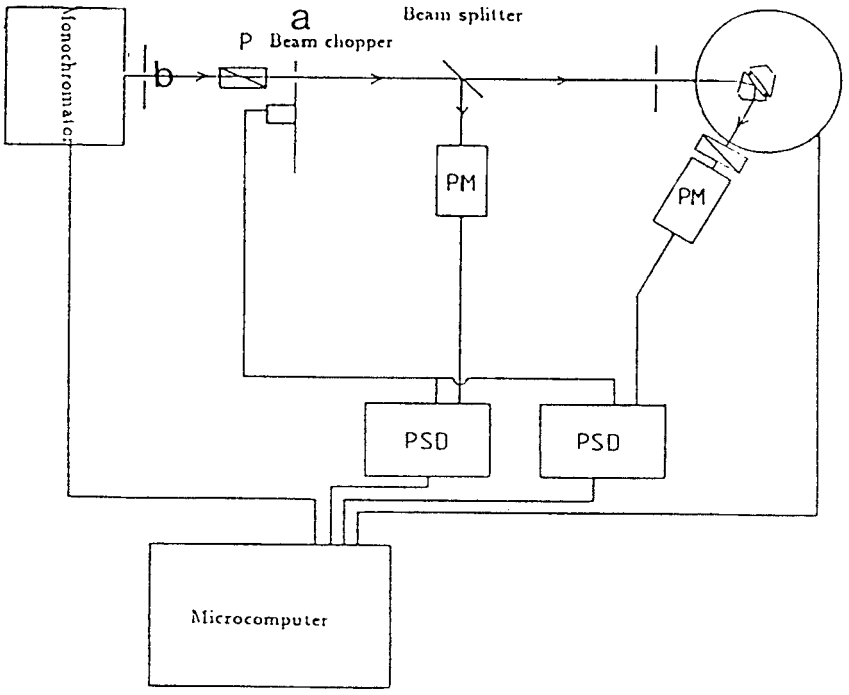

Figure 12. The experimental arrangement for wavelength characterization.

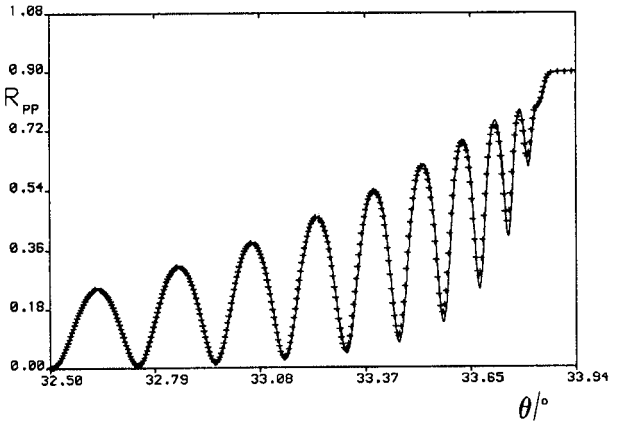

Figure 13. The experimental reflectivity data (+) compared with theory (——) for data taken on an unfilled cell with TM-polarization at 632·8 nm.

At each stage of deposition reflectivity measurements allows us to determine the optical parameters. The results for typical ITO coated pyramid system filled with air is shown in figure 13. The good quality of the comparison was obtained by including a gaussian spread in the thickness ($\sigma = 0{\cdot}1\ \mu$m) and a slight angle spread in the incident beam ($\sigma = 0{\cdot}0105°$). The ε values of the ITO,

$$\varepsilon = \varepsilon_R + i\varepsilon_I = 3{\cdot}591 + i0{\cdot}4$$

Downloaded At: 12:36 26 January 2011

may be related to n and k by

$$\varepsilon=(\varepsilon_R+i\varepsilon_I)=(n+ik)^2$$

giving

$$\varepsilon_R=n^2-k^2$$

and

$$\varepsilon_I=2nk.$$

In this way the n and k values for each overlayer of material may be found. For indium tin oxide the refractive index as a function of optical wavelength falls on a Cauchy dispersion curve of the form

$$n=A+B/(\lambda/\mu\text{m})^2+C/(\lambda/\mu\text{m})^4$$

where $A=1{\cdot}46655\pm10^{-5}\,\mu\text{m}^{-2}$, $B=0{\cdot}18742\pm10^{-5}\,\mu\text{m}^{-2}$ and $C=-0{\cdot}01195\pm2\times10^{-5}\,\mu\text{m}^{-4}$ [7].

The prism-coupling method may also be used to obtain the wavelength dependence of the refractive index for the polymer alignment layer and the polymer index may be described by a Cauchy dispersion formula of the form

$$n=A+B/(\lambda/\mu\text{m})^2+C/(\lambda/\mu\text{m})^4,$$

where $A=1{\cdot}67996$, $B=0{\cdot}02270\,\mu\text{m}^{-2}$ and $C=3{\cdot}7\times10^{-3}\,\mu\text{m}^{-4}$. For a cell filled with the ferroelectric liquid crystal MIX 783 a good comparison is obtained between the experimental data and theory. A typical set of data is shown for TE modes taken in the vertical orientation (in figure 14) at room temperature with light incident at 550 nm.

We have obtained good quality fits across the entire wavelength spectrum with:

(i) a uniaxial slab model with no optical dielectric biaxiality in the system;

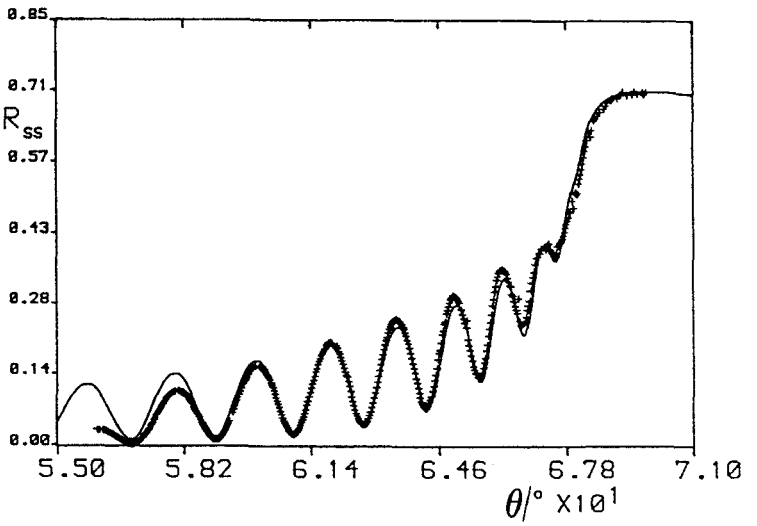

Figure 14. The experimental reflectivity data (+) taken at 550 nm compared with theory (——) for a 3·5 μm cell of MIX 783 for TE-polarization with the optic axis perpendicular to the plane of incidence.

Downloaded At: 12:36 26 January 2011

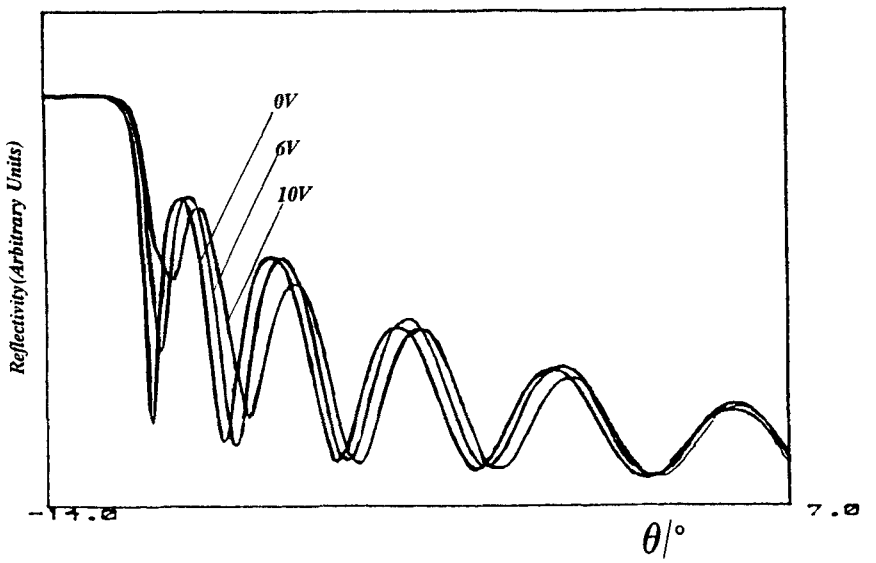

Figure 15. Typical experimental reflectivity curves as a function of applied DC voltage in the forward biased direction for the ferroelectric liquid crystal SCE 8 taken at room temperature for TE-polarization with the optic axis perpendicular to the plane of incidence.

Downloaded At: 12:36 26 January 2011

(ii) no dispersion with wavelength of the in-plane tilt angle, the physical structure remains constant with the wavelength of probe light, this is consistent with the results of other workers [10];

(iii) there is purely dispersion of the refractive indices with wavelength. The Cauchy dispersion formula of this material for n_e^2 has the form given previously with $A=2{\cdot}51552$, $B=0{\cdot}16035$, $C=0{\cdot}01818$. The Cauchy dispersion formula of n_0^2 has the same form with $A=1{\cdot}96282$, $B=0{\cdot}29592$ and $C=-0{\cdot}02661$.

6. Optical mode characterization under an applied electric field

The optical guided mode dielectric responses of MIX 783 and SCE 8 were investigated by applying DC voltages across ITO conductive layers. Perturbations of the experimental reflectivities as a function of low applied DC voltage were compared to those predicted by the model, this allowed us to evaluate the optic tensor. Typical data as a function of the DC forward biased applied electric field is shown in figure 15 for the ferroelectric liquid crystal SCE 8. Comparing data at different applied voltages reveals that all mode positions are no longer coincident with their zero voltage counterparts. Comparison of theory with experiment indicated there is a region of liquid crystal in the middle of the cell largely undistorted under an applied electric field consistent with the retention of the chevron structure [16]. It is necessary that a singular point exists for the continuity of the director field in the centre of the cell giving rise to a chevron interface.

6.1. *Developing the in-plane/out-of-plane tilt profiles*

Since there is a lack of theory to describe adequately a distortion within a ferroelectric liquid crystal layer, an analogy to the nematic case will be considered. For

a parallel aligned nematic cell a reasonable first approximation to the out-of-plane tilt under an applied electric field is given by

$$\tau(z, V) \approx \arctan(A(V)) \sin(z\pi/d)),$$

where z is the position through the cell, d is the cell thickness and A is some function of V applied rms electric field. It has also been observed that in a nematic liquid crystal a surface anchoring term should be included to model data adequately by the introduction of imaginary surfaces outside the actual cell [3], this leads to a tilt profile of the form

$$\tau(z, V) \approx \arctan(A \sin(z(\pi - B)/d + B)),$$

where B controls the imaginary separation of the surfaces of the cell. A similar form for the out-of-plane tilt may be used for each half of the ferroelectric liquid crystal cell. It is necessary to introduce a scaling factor for the out-of-plane tilt since the maximum value is not 90°. The resulting form for the tilt in each half of a chevron cell is then

$$\tau(z, V) = (2/\pi)C \arctan(A \sin z(\pi - B)/d + B)),$$

where $(2/\pi)C$ controls the maximum value of the tilt, and d is now half the cell thickness. The calculation of out-of-plane tilt repeats with a reverse of sign of tilt in the second half of the cell. If $B = 0$ the surface anchoring energy is infinite but if $B = \pi/2$ then the surface anchoring energy is zero. The region over which the pinned point was influential was increased by squaring the sine term to give

$$\tau(z, V) = (2/\pi)C \arctan(A \sin^2(z(\pi - B)/d + B)).$$

It is necessary to calculate the theoretical optical reflectivity curves of a ferroelectric liquid crystal cell for different optic tensor profiles in order to compare them with the data and hence determine the best model. A least squares fitting routine (NAG E04JAF) allowed variation of the parameters A, B and C. The optical calculation was carried out by splitting the liquid crystal layer into 91 sub-layers and calculating the in-plane/out-of-plane tilt for each of these sub-layers and then generating the theoretical reflectivity curve. By allowing this program to compare theory with the data the best values of the A, B and C parameters were obtained.

Slight discrepancies are observed between the theoretical predictions and experimental reflectivity data, but this is not surprising since the form for the out-of-plane tilt is purely empirical and is not based on theoretical continuum mechanics for the ferroelectric liquid crystal. Even the simple nematic case with three elastic constants does not generally lead to simple analytic forms for the in-plane/out-of-plane tilt, so the analytic forms presented here will not be perfect. A good fit is shown in figure 16 for the ferroelectric liquid crystal MIX 783 at room temperature with 2 V applied to the system for Rss in the vertical orientation, the form for the in-plane tilt comes directly from the previous calculation of the out-of plane tilt and is given by de Vos *et al.* [17] as

$$\chi = \arctan(\tan^2(\theta) - \tan^2(\delta - \text{abs}(\tau))^{0.5},$$

where abs(τ) refers to the absolute value of the out-of-plane tilt. Tilt profiles as a function of DC applied voltage are given in figure 17. It is clearly observed that the modelled bulk in-plane tilt and bulk out-of-plane tilt increase in the cell as the applied voltage is increased, approaching the cone angle for the material in the high voltage limit, as expected. It is also observed that there is still an effective boundary region on the application of a DC voltage which is consistent with our zero voltage results. The

Downloaded At: 12:36 26 January 2011

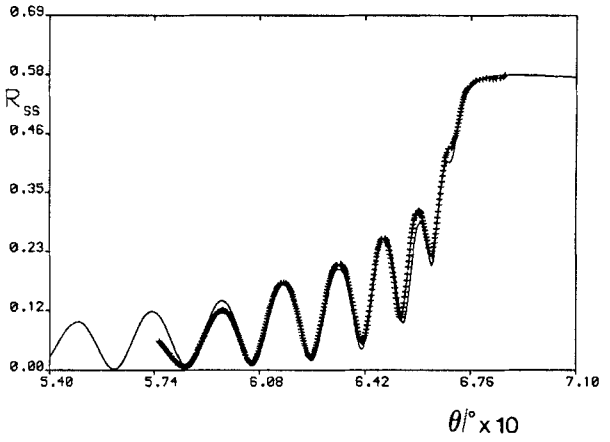

Figure 16. Experimental reflectivity data (+) compared with theory (——) for the material MIX 783 at room temperature with 2 V DC applied in the forward biased direction for TE-polarization with the optic axis perpendicular to the plane of incidence.

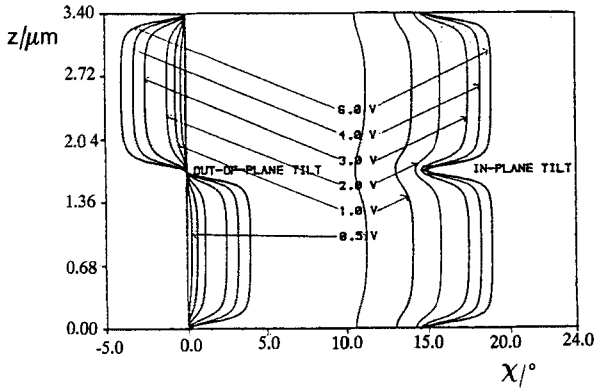

Figure 17. Tilt profiles for the material MIX 783 as a function of applied DC voltage in the forward biased direction.

out-of-plane surface tilt profile decreases rapidly upon the application of a small DC voltage and correspondingly the in-plane surface tilt profile χ_0 increases significantly. For greater than 3 V changes in both the surface tilt profiles are not significant. For voltages in the range $1 < V \leqslant 6$ there is weak pinning of the in-plane tilt in the middle of the cell which does not quite maintain the original zero voltage in-plane tilt value. Strong pinning would maintain the in-plane tilt of the central region at its zero voltage value. As the applied voltage is increased the boundary regions decrease in width, this is consistent with the permanent dipoles reorienting under the application of an applied electric field. For voltages greater than 6 V some distortion in the layering occurs, our simple layer model is then no longer able to achieve good comparisons between theory and experiment.

7. Summary

(i) The optical probing technique is a useful experimental technique for the analysis of thin layers.

Downloaded At: 12:36 26 January 2011

(ii) We achieved an optical verification of the chevron in the layering detected by Clark and Rieker [11] using more conventional X-ray scattering experiments. The simple uniaxial model of the optical dielectric tensor is sufficient to fit the data both with nematic ordering and the imposition of S_A layering.

(iii) If thin boundary regions are introduced at the polyimide/liquid crystal interfaces then similarly good fits are obtained for all sp-mixed experimental data in the S_C^* phase. The prism-coupling optical technique is sufficiently sensitive to probe this boundary layer region.

(iv) The sharp sp-mixed Fabry–Perot resonances in incident angle may yield a high contrast switching element as a function of DC applied electric field if operated near a resonant feature. As the voltage is applied and increased it is possible to sweep through the resonance and thereby alter the detected reflectivity.

(v) A uniaxial model in the optical dielectric tensor for MIX 783 is sufficient to model all the data across the visible region of the spectrum (450–750 nm). Useful information regarding the wavelength response of these typical ferroelectric liquid crystals and thin film overlayers has been shown.

(vi) Distortion of the optic tensor of a ferroelectric liquid crystal under an applied DC voltage in the forward biased condition was also investigated and an empirical form for the out-of-plane tilt gave good agreement with low voltage data requiring a pinned point or chevron interface in the modelling, again consistent with the X-ray scattering results. The results and modelling of this data give much needed information as regards the layer structure in chevron ferroelectric liquid crystal cells and the layer distortion as a function of applied voltage occurring in this class of electro-optic device.

Downloaded At: 12:36 26 January 2011

Much useful discussion was shared between the author and Professor J. R. Sambles of Exeter University, Dr S. J. Elston of Oxford University and Dr E. P. Raynes, F.R.S. and M. J. Towler of RSRE Malvern.

References

[1] Otto, A., 1968, *Z. Phys.*, **216,** 398.
[2] Kraetschmann, E., and Raether, H., 1968, *Z. Naturf.* (*a*), **23,** 2135.
[3] Welford, K. R., 1986, Ph.D. Thesis, University of Exeter, England.
[4] Lavers, C. R., and Sambles, J. R., 1990, *Liq. Crystals*, **8,** 557.
[5] Lavers, C. R., and Sambles, J. R., 1991, *Ferroelectrics*, **113,** 339.
[6] Lavers, C. R., Cann, P. S., Raynes, E. P., and Sambles, J. R., 1991, *J. Mod. Optics*, **38,** 1451.
[7] Lavers, C. R., and Sambles, J. R., *Jap. J. appl. Phys.*, **30,** 729.
[8] Berreman, D. W., and Scheffer, T. J., 1970, *Phys. Rev. Lett.*, **25,** 577.
[9] Azzam, R. M. A., and Bashara, N. M., 1979, *Ellipsometry and Polarised Light* (North-Holland), p. 200.
[10] Ko, D. Y. K., and Sambles, J. R., 1988, *J. opt. Soc. Am.* A, **5,** 1863.
[11] Clark, N. A., and Rieker, T. P., 1987, *Phys. Rev. Lett.*, **59,** 2658.
[12] Pelzl, G., 1979, *Molec. Crystals liq. Crystals*, **53,** 167.
[13] Anderson, M. H., Jones, J. C., Raynes, E. P., and Towler, M. J., 1991, *J. Phys.* D, **24,** 338.
[14] Elston, S. J., *Liq. Crystals* (to be published).
[15] Lavers, C. R., Sambles, J. R., Raynes, E. P., and Cann, P. S., 1992, *Liquid crystals* (submitted).
[16] Elston, S. J., and Sambles, J. R., 1991, *Ferroelectrics*, **113,** 325.
[17] de Vos, A., Reynaerts, C., and Cuypers, F., 1991, *Ferroelectrics*, **113,** 467.